A SERIES OF LECTURES ON OPERATIONAL PHYSICS OF POWER REACTORS

P. MOHANAKRISHNAN, B.P. RASTOGI
Bhabha Atomic Research Centre,
Bombay,
India

ABSTRACT

This report discusses certain aspects of operational physics of power reactors. These form a lecture series at the Winter College on Nuclear Physics and Reactors, Jan.- March 1980, conducted at the International Centre for Theoretical Physics, Trieste, Italy. The topics covered are (a) the reactor physics aspects of fuel burnup (b) theoretical methods applied for burnup prediction in power reactors (c) interpretation of neutron detector readings in terms of adja cent fuel assembly powers (d) refuelling schemes used in power reactors. The reactor types chosen for the discussion are BWR, PWR and PHWR.

1. FUEL BURNUP EFFECTS

In power reactors the fuel and core structural materials are irradiated for a period of few years. This leads to changes in the mechanical, chemical and physical behaviour of these materials with time. Here we will be concerned mainly with the physics aspects of irradiation of fuel only. The important effects are (i) Energy production, (ii) Changes in fuel composition and fission product build up, (iii) Reactivity changes and effects of burnable poisons, (iv) Changes in control rod worth and control rod depletion and (v) Changes in kinetic characteristics.

(i) Energy Production

When fissile nuclei like ^{235}U, ^{238}U or ^{239}Pu absorb a neutron there is some probability of these nuclei fissioning. The fission fragements are emitted within 10^{-14} sec. The fission fragments contain excess of neutrons which are emitted promptly. Within 10^{-11} sec., the prompt γ-rays are also emitted from the fission fragments. Fission fragments then stop in the fuel or cladding. The distance travelled by them is $\approx$ 0.1 mm. They continue to be β^- active to reduce the neutron to proton ratio to a more stable level. The kinetic energy of the fission fragments and all these radiation energies add up to the energy released by a fission.

Some of the neutrons are captured by the fuel and also by other materials like clad and moderator leading to γ-ray emissions. This also contributes to the energy production in reactor. But the anti-neutrinos emitted with decays are lost. Neutron capture energy release is evidently reactor dependent. The energy effectively deposited per fission have thus been evaluated by Unik and Gindler (1971), by comparing the masses of reactants and products, adding the radi- ative capture energy and removing the antineutrino energy. Their evaluations are presented in Table-I. It is seen that higher mass numbers leads to higher fission energy release. Out of this total energy deposited in the reactor only 96 to 97 percent appear as heat energy in the fuel and clad to be removed by the coolant. Three to four percent of the energy is deposited in the moderator directly by the γ-radiations and due to neutron solwing down.

(ii) Changes in Fuel Composition and Fission Product Buildup

Heavy nuclides get depleted due to fission. They get transformed to other heavy nuclides by neutron capture, radioactive decay and (n, 2n) reactions. The build up and decay chains of the heavy nuclei are presented in Fig.1.

Majority of the nuclides disintegrate only by α-emission. Only α-decay half lives less than 500 years are mentioned in the figure. Two important beta decaying nuclides usually found in reactors are ^{233}Pa and ^{241}Pu. Since ^{233}Pa is an absorber its somewhat long half life compared to ^{239}Np leads to some limitations on neutron flux level in the Th - ^{233}U fuel cycle compared to U - ^{239}Pu fuel cycle. Similarly the loss of ^{241}Pu and build up of absorber ^{241}Am with time lead to loss of reactivity in Pu fuelled reactors operating at low neutron flux level or power level.

The spontaneous fission half lives of the nuclides are not noted here. Important examples are ^{242}Cm, ^{244}Cm, ^{242}Pu and ^{240}Pu. The number of spontaneous fission neutrons emitted/gm/sec for ^{242}Cm is $\approx 2 \times 10^{7}$ while that for ^{240}Pu it is $\gtrsim 1 \times 10^{3}$.

Approximate Beginning of Life (BOL) and End of Life (EOL) fuel compositions in BWR and PHWR are given in Table-II.

Fission products

Fission fragments and their decay products are known as fission products. Their masses are in the range 80 to 160. There are five areas where the information about fission products becomes necessary in reactor physics of power reactors.

a) Multiplication factor and power distribution prediction with burnup,

b) Measurements of burnups,

c) Estimation of delayed neutron fraction,

d) Prediction of decay heat output of fuel after reactor shut down and

e) Radioactivity of irradiated fuel.

Now we will consider the fission products only from the interest in first area. Enormous amount of efforts have been made to determine the fission yields and cross-sections of the fission products. For example latest compilation of fission yields have been made by Cuninghame (1977) and Rider (1978). About a hundred fission products have appreciable yield-multiplied by-cross-section values. About 30 of them account for 90% of the total absorption by fission products in the burned fuel.

To quote an example, let us consider the well-known case of ^{135}Xe. The full chain of ^{135}Xe production in reactor is given in Fig.2. It is conventional to consider a simplified chain for finding the ^{135}Xe concentration in the reactor

$$^{135}I \xrightarrow[6.61\ hr]{} {}^{135}Xe \xrightarrow[9.08\ hr]{} {}^{135}Cs \text{ (non absorbing)}$$

The text book expressions for ^{135}Xe concentrations can then be easily derived. It can then be shown that the Xe concentration is higher for higher flux levels and that Xe concentration reaches a maximum after reactor shut down beyond flux levels of the order of 10^{12}. It has been shown by Ottewitte (1977) recently that for flux levels of 4×10^{14} n/cm^2/sec this maximum concentration of Xenon after shut down can be underestimated by $\gtrsim 10\%$ if the whole chain given in Fig.2 is not considered. The important extra chain to be considered is the formation of metastable ^{135}Xe.

Examples of highly absorbing fission products which lead to stable and very less absorbing products are ^{113}Cd, ^{157}Gd and ^{149}Sm. Another isotope which shows flux dependent concentrations like Xenon is ^{105}Rh. But, while the Xenon absorption worth is about 0.02 to 0.03 $\Delta k/k$ for thermal reactors fuelled by natural or enriched uranium, the absorption worth of ^{105}Rh is about one order of magnitude smaller.

Units used for specifying burnup

Before going further, I would like to discuss about the units used in quantifying burnup in power reactors.

Three type of units have been used to quantify the burnup of any nuclear fuel. These units result from points of view that look at burnup in three different ways.

i) In terms of energy produced from fuel,

ii) In terms of atoms destroyed by fission/initial concentration of heavy atoms, and

iii) In terms of time integrated neutron flux in fuel

The first one is the most popular approach in LWRs and fast reactors. Burnup is expressed in units of Watt Days/gm or MegaWatt Days/tonne. The heat energy produced in the reactor can be accurately estimated by enthalpy balance (provided proper pressure and temperature monitoring is present). This in MegaWatt Days is divided by the total weight of fuel to give the average burnup of fuel. To find the burnup distribution we usually have to depend on either calculated or measured power distribution. It is conventional to use the weight of only the metal part of oxide fuel in LWRs for expressing the burnups.

Experimental measurements of burnup depend on the measurement of concentration of fission products or of radioactivities left in the fuel. Consequently burnups are expressed in units of percentage fissions per initial metal atom. To convert this to WD/gm we first determine the number of fissions in 1 gram of fuel. Then knowing the energy absorbed in reactor/fission of each of the nuclides the burnup in Watt Days/gm can be estimated. It is evident that for this, the number of fissions in each of the isotopes is to be known separately.

Burnup in terms of neutron irradiation has been conventionally used in case of PHWRs. The amount of irradiation or fluence is specified in units of neutron/kilo barn. Fluence or flux multiplied by time can be converted to number of fissions in the fuel if the macroscopic cross-section of the fuel at any burnup is known. Thus the convertion of burnup expressed in terms of irradiation to MWD/tonne will depend heavily on calculated values of macroscopic cross-sections with burnup.

(iii) Reactivity Changes

We shall consider the changes in multiplication factor of typical LWR fuel and of PHWR fuel.

In Fig.3 we give the plot of k_∞ variation with burnup of PHWR fuel having enrichment 2.4% and moderator to fuel volume ratio 2.3. As described by earlier lectures the water inside the fuel channels boil. So we have plotted the k_∞ for two cases - a zero steam case and the other for 0.7 volume

fraction of steam, generally termed void fraction. The water densities in the two cases are 0.74 and 0.25 gm/cc, respectively. The fuel assembly consisted of a 6 x 6 array used in TAPS reactors, India.

The k_∞ for zero steam volume fraction reduces from 1.281 to 1.245 just at the zero burnup itself due to build up of Xenon. Rest of the k_∞ computations upto 25 GWD/Short tonne (one short tonne = 2000 lbs) used an equilibrium concentration of Xenon corresponding to the average fuel assembly power in reactor. It is to be remembered that this worth of Xenon is power (flux) dependent. So proper corrections are to be applied to these k_∞s for fuel which is operating at lower or higher than the average rated power. After this initial sudden dip, the k_∞ falls monotonically with burnup due to the depletion of fissile material and build up of fission products. The rate of fall of k_∞ slows down at higher burnups due to the increased production of ^{239}Pu and ^{241}Pu per fission of a thermally fissile isotope.

Since the neutron spectrum is harder at higher steam volume fractions the k_∞ at zero burnup is lower by about 40 mK for 0.7 void case compared to the 0 void case. But the harder spectrum leads to higher ^{238}U conversions. This finally results in k_∞s in the 0.7 void case to be higher than the 0.0 void case at high burnups of the fuel.

The effect on introduction of burnable poison in two of the 36 fuel rods (1.5 wt% Gd_2O_3) is depicted in Fig.4. Here the k_∞ values of fuel bundle without and with the burnable poison are plotted for comparison. The worth of Gd_2O_3 at zero burnup is about 0.11 $\Delta k/k$. The k_∞ of fuel with burnable poison initially rises with burnup due to the fast conversion of ^{155}Gd and ^{157}Gd isotopes to nonabsorbing ^{156}Gd and ^{158}Gd isotopes. The k_∞ reaches a maximum around 4000 MWD/St and then falls and merges nearly with the k_∞ of fuel without the burnable poison. Other than the easily recognisable reduction in control requirement brought about by burnable poisons, the use of such bundles can lead to better power flattening during the operation of the reactor. This is illustrated in Fig.5.

Consider the shown combination of two fresh burnable poison bearing fuel bundles and exposed fuel bundles around a control rod. The powers produced by them will be in proportion to their k_∞ values. After about 4500 MWD/St burnup in a cycle, the distribution of k_∞ values have changed such that the roles of adjacent bundles are interchanged. Two of the bundles are gaining in k_∞ while two bundles are loosing in k_∞. It is thus evident that around half of this burnup step, all the four fuel bundles would be producing nearly the same power. The net effect relative to the case of fresh bundles with no burnable poison is the reduction in mismatch of k_∞ values between adjacent fuel bundles and consequent reduction in power mismatch.

In Fig. 6 we have depicted the behaviour of infinite multiplication factor with burnup of PHWR fuel. It shows more interesting features than that of LWR fuel. There is the sudden dip in k_∞ caused by Xenon build up within a days time of operation. Then k_∞ continues to fall upto abcut 200 MWDs/tonne after which it rises again and reaches a maximum around 1100 MWD/tonnes and then falls monotonically. This interesting behaviour is due to the following reasons. The initial slow fall in k_∞ is due to the build up of ^{239}Np which is an absorber. Subsequently it decays with a half life of 2-3 days to ^{239}Pu. The formation of ^{239}Pu with burnup leads to an increase in K_∞ for PHWR fuel. In thermal energy range, ^{238}U is a major absorber in natural U fuel

used in PHWRs. The formation of ^{239}Pu which has nearly double the absorption cross-section of ^{235}U increases the k_∞ of fuel even though the number of ^{239}Pu atoms produced per one neutron absorbed in ^{235}U is less than unity. Once ^{239}Pu also starts depleting due to fissions, the k_∞ starts falling monotonically.

(iv) Changes in Control Rod Worths and Control Rod Depletions

The ability of a control rod to absorb neutrons depends on its ability to compete with the other neutron absorbers, particularly the fuel. Since the isotopic changes in fuel give rise to changes in absorption cross-section, the worth of control rods can also change. But it turns out that the increase in absorption cross-section expected with ^{239}Pu and fission product formation is more or less compensated by the reduction due to depletion of ^{235}U. In PHWRs the increase in absorption cross-section of fuel is about 25% at discharge burnup. So here also the increases in absorption cross-section of fuel with burnup is not drastic enough to cause significant changes in control rod worths.

Control rod depletion is also not a trivial problem in operating power reactors. For example consider the case of a BWR with control rods made of absorbing material B_4C. It has been generally accepted that about 10% reduction in control rod worth is acceptable in consistency with the uncertainty in control rod worth estimation. It has been found that for cruciform control rods found in BWRs this corresponds to about 40% depletion of the absorber ^{10}B. This may be reached in ten to fifteen years of reactor operation in many portions of different control blades. To avoid large errors in reactivity and power distribution predictions after ten to fifteen years of operation, it is necessary to keep track of control rod depletions along the height of different control blades.

(v) Changes in Kinetic Characteristics

The delayed neutron fractions are different for ^{239}Pu (0.0021) and ^{241}Pu (0.0049) as against that of ^{235}U (0.0065). Thus with fuel burnup of uranium fuel, the delayed neutron fraction reduces from 0.007 to 0.005 in LWRs.

Fuel temperature coefficient is $\approx -1 \times 10^{-5} \Delta k/k$ for LWRs. Magnitude of this increases with fuel burnup due to ^{240}Pu production which has a absorption resonance at 1.06 eV. On the contrary, in PHWRs the magnitude of the fuel temperature coefficient reduces with fuel burnup due to effect of ^{239}Pu fission resonance at 0.29 eV. Due to widening of this resonance with fuel temperature increase, more neutrons are absorbed in ^{239}Pu in preference to ^{238}U. However, in all, fuel temperature coefficient remains negative at any fuel burnup.

In the case of moderator temperature coefficient also LWRs and PHWRs show divergent behaviour with fuel burnup. At the operating temperature, the LWR moderator temperature coefficient is negative at all fuel burnups. But in PHWRs, where the moderator is near room temperature, the moderator temperature coefficient becomes positive starting with a negative value at zero burnup. This is again due to the fact that the hardening of neutron spectrum decreases ^{235}U absorptions but increases ^{239}Pu absorptions.

Even in LWRs the moderator temperature coefficient at any burnup can be positive when large amount of poison like boric acid is dissolved in the moderator.

With fuel burnup, the prompt neutron life time reduces as it is roughly proportional to the inverse of the thermal absorption cross-section of reactor. As mentioned earlier, the increases in absorption cross-sections are only 10% in case of LWRs and 25% in case of PHWRs leading to corresponding reductions in prompt neutron life times.

2. THEORETICAL METHODS FOR CALCULATING BURNUP

(i) Introduction

The present day approach to reactor physics problems is a fairly rigorous one. We start with the basic nuclear data like microscopic cross-sections, radio active decay constants etc. Through a mathematical model coded into complex computer programs arrive at informations required for reactor operation like the power distribution or fuel burnup distribution. A satisfactory model of the fuel burnup process must represent the isotopic changes in each point of the power reactor and the consequences of these changes. This calls for the solution of the neutron transport problem as well as the solution of the equations governing fuel isotopic changes (burnup equations). Evidently the task is a very stupendous one.

One part of the task is to evaluate the neutron spectrum and its magnitude throughout the three-dimensional reactor. Due to the geometric complexity involved, this problem is not amenable for direct solution even in modern computers. The approximation usually introduced is the separation of local fuel element effects and the global reactor effects. This enables the calculations to be performed in two stages.

A fuel element in two dimensions forms the basis of the reactor lattice and is called the lattice cell or fuel cell. The analysis of such a fuel element alone to find the neutron spectrum is called the lattice cell calculation stage. Here the assumption that the reactor consists of an infinite array of such fuel elements is used.

Calculations are performed using the neutron transport equation and in many neutron energy groups. The neutron leakage from the core and the effect of fuel cell differences and the exact magnitude of neutron fluxes in different cells are found in the core calculation stage. Condensed information from the lattice cell calculation stage is fed to the core calculation stage. Core calculations are normally performed in a few neutron energy groups and using diffusion equation.

Luckily the time constant for fuel burnup $\left(\frac{1}{\sigma\phi}\right)$ is of the order of months. Hence the lattice cell calculations and the core calculations are static calculations. Except for the effects produced by Xenon, the fuel nuclear properties can be held to be invariant for a period of 2 to 4 weeks or more for fuel burnup evaluations. Hence only repetitive solution of the static problem is required as a function of time. To reach one static problem from the earlier, the solution of burnup equations are required to be carried out.

The build up, decay and transformation of different heavy nuclides and fission products are governed by coupled first order differential equations. Solution of these equations with appropriate cross-sections and neutron flux levels gives the isotopic compositions

at different points of the reactor. Due to the break up of the reactor calculations into two stages, there exists two schemes in which the integrations of these equations can be carried out. The integration of burnup equations may be performed at the cell calculation stage or core calculation stage.

(a) Burnup equation integration at the lattice cell calculation stage

For reactors for which the basic separation of lattice and core calculations is a good approximation i.e., the local spectrum is insensitive to environment, the integration of burnup equations can be carried out at the cell calculation stage. This can be done for PHWRs and BWRs. In PHWRs the presence of large amount of D_2O moderator and the large size of the reactor make the above separability assumption valid. The water gaps separating fuel bundles in BWRs is believed to shield the effects of envirnoment. Recent investigations of Zolotar (1979) confirm this point of view. In this scheme, we obtain the macroscopic cross-sections as a function of fuel burnup and moderator conditions in the lattice cell calculations. Fuel isotopic compositions at different burnups are also generated. Core calculations are performed with the macroscopic cross-sections. The power distributions and fuel burnup at different points (nodes) of the reactor are obtained from the core calculations. To get the fuel isotopic composition of any fuel in the reactor, interpolations in the fuel composition data prepared at the lattice calculation stage would be required.

(b) Burnup equation integration at the core calculation stage

In those situations where the properties of neighbouring fuel bundles affect the neutron spectrum in a given fuel bundle, it is desirable to perform the integration of burnup equation at the core calculation stage. This is evidently the more realistic approach. This scheme has been popular in PWR reactor analysis. Here, in the lattice cell calculation stage we derive microscopic cross-sections as a function of isotopic composition of fuel (composition changes produced by burnup) in a few neutron energy group structure. Subsequently core caloulations are carried out with macroscopic cross-sections prepared using the actual fuel compositions and the above mentioned microscopic cross-sections. The few neutron energy group spectrum obtained by the core-calculations in each of the fuel bundle is then used to compute the reaction rates in different isotopes and hence the changes in fuel composition. The core calculations may be performed In such a scheme, only in two-dimensions over the radial plene of the reactor. The axial variation of flux is treated by buckling (B^2) approximation or by flux synthesis in more sophisticated codes.

(ii) Fuel Burnup Calculations in a BWR

As an example we will consider the application of the former scheme mentioned in last section, which we have successfully implemented in India. We are using such a scheme since 1976 for the fuel management of Tarapur BWRs.

The unit cell of the BWR reactor lattice is shown in Fig. 7. It consists of 36 fuel rods of three different enrichments. Two of the fuel rods contain Gd_2O_3 as burnable poison. In the wide water gap, cruciform control rod as shown in the figure may be present. Instrument tube is usually located at the narrow-narrow water gap corner.

In the cell calculation stage, our basic problem is to calculate the reaction rate in each of the isotopes in every pin in this unit cell. Number of absorptions in isotope 'i' in one of the fuel pins Ra^i is given by (for number density N_i)

$$R_a^i = \int_0^{10\ MeV} N_i\ \sigma_a^i(E)\ \phi(E)\ dE$$

here $\sigma_a^i(E)$ is the microscopic absorption cross-section of isotope 'i' for neutron energy E and $\phi(E)$ is the neutron flux in the fuel pin of interest at energy E. However, we perform the above integration indirectly. Let $\overline{\sigma_a}$ and $\overline{\phi}$ denote one group absorption cross-section and flux such that the reaction rate is given by their product

$$R_a^i = \overline{\sigma_a}^i\ \overline{\phi}\ N_i$$

where $\overline{\phi} = \int_0^{10\ MeV} \phi(E)\ dE$ is the total flux.

Hence $$\overline{\sigma_a}^i = \frac{\int \sigma_a^i(E)\ \phi(E)\ dE}{\int \phi(E)\ dE}$$

To perform the fuel burnup calculations our aim is thus to determine the effective one group cross-sections for each of the isotopes in every pin and the total flux level in every fuel pin.

(a) Lattice cell model

Major steps in the lattice cell calculation stage are shown in Fig. 8. The 69 neutron energy group WIMS library of U.K. is the source of microscopic cross-sections of all isotopes in the lattice cell. In the library condensation stage a microscopic cross-section library in 28 groups is prepared using typical spectra in a light water lattice cell. Both the libraries give importance to the 0.29 eV and 1.06 eV Pu isotope resonances for fixing the energy limits of groups.

Macroscopic cross-sections of each material in the fuel box are prepared using this 28 group library taking into account its isotopic composition.

One fuel pin, its can and surrounding moderator constitute a pin cell. Neutron flux disadvantage factors in this pin cell are calculated using integral transport theory in the Wigner-Seitz cell. For this we have developed a fast and accurate program MURLI based on interface current method. Homogenised pin cell cross-sections are obtained using the disadvantage factors.

Spectra calculated in such a single pin cell do not take into account the effect of heterogeneities like water gap, control rod and adjacent fuel pin differences. Neutron spectra in the whole lattice cell is obtained by what is known as supercell model. The homogenised pin cell cross-sections are used to construct a one-dimensional picture of the fuel box, as homogenised fuel cells surrounded by water gap. This lattice cell in simplified geometry is analysed by integral transport theory (MURLI) to obtain neutron spectra in water gap and different fuel cell rings. Evidently the spectrum in the outer fuel rings will be softer due to the proximity of water gap. The fine structure heterogeneity of the control rod is homogenised by P1 blackness theory approach with the blackness parameters evaluated using an integral transport method. Spectrum changes caused by the presence of

the control rod are evaluated by super cell constructed with the homogenised control rod, stainless steel sheath, water gap and homogenised fuel cells in slab geometry. Similarly spectra in Gd_2O_3 bearing fuel pins are evaluated by constructing mini super cells consisting of Gd_2O_3 bearing fuel pin, associated moderator, surrounding homogenised fuel cells and part of the water gap.

With the neutron spectra in 28 groups derived by the above described super cell model, the macroscopic fuel cell cross-sections as well as the microscopic isotope cross-sections are condensed to five or six neutron energy group structure. With the macroscopic cross-sections two-dimensional calculations of the lattice cell are performed in diffusion theory to obtain the pin cell power distribution and infinite multiplication factor (k_∞).

Neutron spectra were evaluated assuming zero net current boundary conditions in the supercell calculation stage or two dimensional calculation stage. In the reactor, the reactivity excess or deficiency of a lattice cell is taken up by neutron leakage out or into a lattice cell. This leakage effect on neutron spectrum can be represented approximately by performing a criticality calculation with the five or six group homogenised lattice cell cross-sections and adding a DB^2 dependent leakage term where D is the homogenised diffusion coefficient of lattice cell. In some reactor lattices, this leakage between adjacent fuel bundles can not be described by a DB^2 dependence (i.e. higher leakage at higher energies). In such cases, the basic separation of lattice and core calculations is no more valid. To simulate the effect of control absorber present during some part of the burnup, an extra absorber having inverse neutron velocity ($1/v$) dependence of cross-section can be considered along with the leakage term during the criticality calculation. A combination of $1/v$ absorber and DB^2 type leakage has been used by us to perform the criticality calculation of the homogenised lattice cell. Lattice cell spectrum correction factors are thus obtained by comparing the neutron spectrum obtained by homogenised criticality calculation with the spectrum obtained by solving the diffusion equation with sources reduced by K_∞ . One group microscopic cross-sections of each of the isotopes in every pin of the lattice cell is now derived by condensing the five or six group microscopic cross-sections with the leakage corrected spectra.

Burnup equations are now solved in each of the pin cells, given the average power rating of the lattice cell. The equations governing isotope concentration changes can be written for isotope ' i ' as

$$\frac{dN_i}{dt} = \overline{\sigma_c}^{i-1} N_{i-1} \bar{\phi} + \lambda_k N_k - \overline{\sigma_a}^{i} N_i \bar{\phi} - \lambda_i N_i + \gamma_{ij} \Sigma_j \overline{\sigma_f}^{j} N_j \bar{\phi}$$

The first term on RHS represents production due to neutron capture and the second term production due to radioactive decay. The third and fourth terms correspond to loss due to neutron absorption and radioactive decay. The last term is non zero only for fission products. The summation over j runs over all fissionable nuclides and γ_{ij} is the fission yield of isotope 'i' from nuclide ' j '

The magnitude of $\bar{\phi}$ is determined by the average power rating of fuel P_c , the local peak factor L_p of the pin cell 'P' and the fission energy release in that pin cell. We have the power produced

in pin cell P per unit volume as

$$\bar{\phi}_p \times \sum_j N_j \bar{\sigma}_f^j Q_j = P_c \times L_p$$

Here summation over j runs over all the fissile isotopes and Q_j is the energy absorbed in reactor/fission of isotope 'j'. P_c is the power produced per unit volume of fuel.

Hence $$\bar{\phi}_p = \frac{P_c L_p}{\sum_j N_j \bar{\sigma}_f^j Q_j}$$

With the above determined one group cross-sections and total fluxes, the integration of burnup equations are carried out by Runge Kutta method or by the simple trapezoidal rule. In consistancy with the LWR-WIMS scheme we also consider seven fission products. ^{135}Xe and ^{105}Rh are considered separately and their concentrations evaluated using the flux level $\bar{\phi}_p$. Fission products having high thermal neutron absorption cross-section like ^{113}Cd, ^{157}Gd and ^{149}Sm are grouped into one fission product and all the remaining fission products grouped into 4 psuedo fission products of increasing resonance integral as suggested by Nephew(1960).

With the change in composition of fuel, $\bar{\phi}_p$ is reevaluated during the integration of burnup equations. Criticality calculations for leakage corrected spectrum are performed typically at intervals of 500 MWD/tonne.

Burnable poison containing pins are divided into small annular rings to simulate the self shielded burning of Gd isotopes. Hence integration of burnup equations are required to be carried out in each of such rings separately at least for the Gd isotopes with the flux levels of each of the rings.

We go back to the pin cell and supercell calculation stage with the changed fuel composition after certain amount of burnup. In uranium bearing fuel it may be required to update the spectra at small intervals of burnup like 500 to 1000 MWD/tonne in the initial stages of burnup due to the production of Pu isotopes. Later on, burnup steps of upto 5000 MWD/t may be used. As long as burnable poison is present, it is required to update the spectra in such pin cells alone at burnup steps of 500 MWD/tonne.

Lattice cell calculations are repeated for different moderator conditions and with and without the control rod. The results of the lattice cell calculations are the macroscopic one group parameters like K_∞ and migration area (M^2). The fuel isotopic composition and the fuel pin burnups at different average lattice cell burnups constitute another set of results.

Factors for neutron flux monitor reading interpretation are also derived from the lattice cell calculation. We will touch up on them in more detail in a subsequent lecture.

(b) Core calculations

There may be many type of fuel bundles in the reactor core. The one group macroscopic parameters as a function of moderator void, burnup and control and lattice cell type (bundle type) are input to the code for core calculations. In BARC, Bombay, we have developed a one neutron energy group BWR simulator 'COMET-G' which is being regularly used for fuel management of Tarapur BWRs. There are 284 fuel bundles

in the Tarapur core and the core is divided into 24 axial nodes of 6" each, matching with the minimum movement of control rods-in all making 6816 nodes (Fig. 9).

The other necessary inputs to the simulator are reactor power, water inlet conditions, core flow, core arrangement in terms of lattice cell types and burnup in 6816 nodes and the control rod pattern. The flow of calculation in the simulator is indicated in Fig. 10.

One group diffusion theory calculations are performed to determine the power distribution with the initial guess that the power distribution is flat in the core. Bundle inchannel coolant flows and voids are then calculated with this power distribution. Lattice cell parameters of the fuel bundles in the core are interpolated for this void guess, burnup, control etc. We then go again for the solution of diffusion equation to determine the power distribution. Coolant flows and voids are now recalculated for the changed power distribution. This process is repeated until converged power and void distributions are obtained. From the thermal power produced in the reactor-determined by heat balance, the energy produced from fuel in MWD/St is known from the reactor operation history for a period of two to four weeks. Reactor conditions have to be approximately constant during this period. Let ΔE be the core burnup step for the aforesaid period. Then the fuel burnup distribution and burnup weighted void distribution are obtained in the following manner:

$$E_{ijk} = E^{o}_{ijk} + \Delta E \; P_{ijk}$$

$$U_{ijk} = U^{o}_{ijk} + \Delta E \; V_{ijk} \; P_{ijk}$$

E^{o}_{ijk} and U^{o}_{ijk} are the initial burnup and burnup weighted void at axial node k in the fuel bundle at location (i,j) in the core. In the fresh core they are zero for all bundles at every axial height. P_{ijk} and V_{ijk} are the power and void at axial height k of bundle at location (i,j).

The average fuel burnup in 6" section of any of the 284 fuel bundles in the core at any time is thus given by E_{ijk}. Average operating void in any such section over its period of burnup is then given by $\overline{V}_{ijk} = U_{ijk} / E_{ijk}$.

To determine the fuel composition we will have to make use of the average operating void $\overline{V}_{ijk}$ also and interpolate in the table of isotopic composition prepared in the lattice cell calculation stage. You may remember that fuel macroscopic parameters and fuel isotopic compositions were determined as a function of burnup and void fraction.

Control rod depletions are also estimated at the core calculational stage using information generated in lattice cell calculations. From the lattice calculations, in presence of control rod, a factor F giving the number of absorptions in control blade per fission in the controlled bundle is calculated. The power produced in any controlled node of a bundle is derived from the core calculational results, say P_{ijk}. Hence the number of fissions in that node for the period of burnup step ΔE can be estimated.

$$\text{Number of fissions during burnup step } \Delta E = \frac{\Delta E \times P_{ijk} \times W}{\text{Energy release/fission}}$$

W is the weight fuel in short tonne for 6" section of fuel assembly.

Number of absorber atoms (^{10}B) depleted in the 6" section of the control blade controlling that node, say $N_B(\Delta E)$ is then given by

$$N_B(\Delta E) = \frac{\text{Number of fissions during burnup step } \Delta E}{F}$$

Depending on the control rod pattern the depletions in different sections of control blades are thus to be kept track of. The changes in control rod worths due to these depletions are then taken into account in the core calculations. As the control rods get depleted, its effect will first manifest in cases where most of the control rods are inside the core like the cold shut down state and cold criticality state.

3. INTERPRETATION OF NEUTRON FLUX MONITOR READINGS

(i) Introduction

Earlier lectures had given you a description of the instrumentation used in neutron flux measurements. In these instruments the response is proportional to the reaction rate produced by the local neutron flux in the detector. In case of fission ionisation chamber it is the number of fissions produced in highly enriched ^{235}U coating and for activation detectors like Vanadium, it is the number of absorptions in that activation material.

Interpretation of the readings of the instrument during power operation of a reactor essentially means relating the adjacent fuel assembly powers from the readings. Fuel assembly powers so obtained are often referred to as "measured powers" . It is evident that some dependence on calculated fuel parameters are required to arrive at these "measured powers" from detector readings. However, these measured powers are used by plant operators to arrive at power shape and thermal hydraulic parameters.

The basic steps followed in the interpretation neutron flux monitor reading are listed in Fig. 11. Measured readings (R) are converted to adjacent fuel assembly power (P) using the ratio (D) of rate of fissions in the fuel assembly to detector reaction rate obtained at the lattice cell calculation stage. $P = kRD$ where k is a proportionality constant. The product RD is only proportional to the fuel assembly power due to the arbitrariness of the detector reading introduced by factors like depletion of detector material, amplifier gain in the electronic circuit etc. Next step is the derivation of values proportional to powers in unmonitored fuel assemblies by making use of symmetry of core loading and extrapolations. The reactor power is known from heat balance. The 'measured' fuel assembly powers are now computed by normalising the sum of above derived values to the reactor power. This information about power distribution is now condensed to give 'measured' power peak parameters and thermal hydraulic parameters limiting the reactor operation. These steps may be coded into a process computer for on line monitoring of power distribution and power shape indices.

Procedures similar to this have been used in the interpretation of detector readings in PWRs and BWRs. The procedure proposed to be used for the Canadian CANDU- PHWRs is slightly different. Early designs of CANDU reactors did not have any detectors for on-line flux monitoring.

It has become evident that accurate on line flux maps would be extremely useful for large reactors like that at Bruce. Here also, factors relating the detector reading to average flux in the node of the size used in core calculations, are derived at the lattice cell calculation stage. The three dimensional power distribution is however deduced in a different manner. The flux distribution $\phi(\underset{\sim}{r})$ is expanded in terms of S realistic flux shapes (modes)

$$\phi(\underset{\sim}{r}) = \sum_{l=1}^{S} a_l \psi_l(\underset{\sim}{r})$$

Let there be detector readings available from R locations in the core $(R > S)$. The coefficients a_l are determined by demanding that the flux $\phi(\underset{\sim}{r})$ should reproduce these readings as closely as possible by a least square method. Typically S= 25 and R =100 are used. Then the fluxes at about 1000 points of interest in the reactor are derived from $\phi(\underset{\sim}{r})$.

(ii) Interpretation of Travelling Incore Probe (TIP) Readings in a BWR

In the following part of the lecture we will consider the different steps for getting measured power distribution in a little more detail. For that, we will consider a specific case- that of a BWR.

The detectors used in obtaining detailed power map in a BWR are called Travelling Incore Probes (TIP). They are located at the water gap intersections of fuel lattice cells. So they monitor the flux level in the water gap corner as contributed by the adjacent four fuel assemblies. Location of these detectors in the radial plane of a BWR is shown in Fig.12. The detector can travel parallel to the axis of the reactor in these locations. 13 such locations are shown here. So the TIP_{system} can monitor 13 x 4 fuel assembly powers directly.

In a BWR, the burnup distribution of fuel bundles in any core loading is desired to be quarter-core symmetric. Further, during reactor operation, the control rod patterns are also maintained quarter core symmetric. Hence the assumption is often made that the TIP reading in any one of these locations is representative of three symmetric locations in other quadrants also. Evidently the validity of this assumption depends on the accuracy of calculated fuel burnups. Believing that our fuel burnup predictions are reasonably accurate, the monitored region of the core can be extended upto the shaded boundary shown inside the core. The fuel lattice cells outside this shaded boundary are not monitored at all. Since they are in the periphery, we can assume that power peaks will not occur there during normal reactor operation.

Correlation of detector fissions to assembly powers

The TIP detector consists of an ionisation chamber inside which a very thin coating of uranium oxide, enriched in ^{235}U in excess of 90%, is present. Fission fragments from the fissions produced in the coating cause ionisation and give rise to a current proportional to the number of fissions produced in this coating.

Our problem in the lattice cell calculation stage is to calculate the number of fissions in this detector material for a given fission power in the adjacent fuel assemblies. Let us call this factor as 'D'. It is assumed that 'D' factor depends only on the burnup of the fuel bundle and the moderator condition inside the fuel channel facing the detector location at that height of the reactor. This is justified by the fact that influence of adjacent fuel cells in a given fuel cell spectrum is not significant. The effect of environment is only to produce a

general increase or decrease of the total flux level over the whole of the cell which will manifest as an increased magnitude of the TIP reading. In short, the D factors are calculated considering only one fourth of the detector and assuming zero net current boundary on all sides of the lattice cell.

Cross-sections of the detector material are prepared in 28 groups and condensed to five or six groups using the spectrum generated in water-gap during the super-cell calculation of the lattice cell (supercell model was discussed in the last lecture). It is now assumed that the detector does not perturb the neutron spectrum adjacent to it. Five or six group fluxes at the corner of the water gap are generated in the two-dimensional diffusion theory calculation of the fuel lattice cell. The condensed fission cross-section of the detector material obtained after the super cell calculation is used to multiply these fluxes to get the number of fissions in the detector material. The amount of detector material considered is immaterial as the D factors are only relative. Further , the fluxes at the water gap corner are obtained by normalising the power produced in the lattice cell to a fixed value. The D factors are given by the fissions in the detector using the same amount of detector material and for a fixed power produced in the lattice cell for different fuel burnups and inchannel moderator conditions.

When control rods are present adjacent to one or more fuel cells surrounding a TIP location, the power sharing between the four cells are to be readjusted taking into account the flux tilt produced by the control rod. The factors for obtaining the readjusted power distribution are derived from four-lattice-cell calculations in the presence of control rod. These factors are found to be nearly independent of burnup and void in the four fuel cells.

Extrapolation to unmonitored assemblies and normalisation

Measured detector readings are thus converted to values proportional to fuel assembly powers at different axial heights using the factors derived from two dimensional lattice cell calculations considering one or four lattice cells. For choosing the proper factors for each of the monitored fuel assembly heights (nodes), we have to depend on the calculated values of burnup and operating instantaneous void at these nodes. These are available from the core calculations.

The calculated voids are consistent only with the calculated power distribution. In a BWR, the thermal hydraulic parameters are critically dependent on the in channel instantaneous voids. To evaluate more realistic power peak parameters the flow of calculations take a more complicated route as shown in Fig. 13 for a BWR.

Values proportional to fuel assembly powers at all axial nodes of directly monitored assemblies are first derived using D factors which are obtained by interpolating with the calculated burnups and voids in these nodes. Using quarter core symmetry, these values proportional to powers in nodes are assumed to be representative of powers in fuel assemblies symmetrically located in the other three quadrants. For normalisation, only the total reactor power is known. A guess will have to be made of the powers in assemblies in the unmonitored region. It is assumed that the total power produced in the unmonitored region is P_F. This is about 0.15 in the case of reactor

shown in Fig. 12. If P_T is the reactor thermal power, the power produced in the monitored region demarcated in Fig.12 is $(1-P_F)P_T$. The factor P_F is derived from calculations using typical core configuration. Due to the fact that power produced in periphery assemblies is governed mainly by neutron leakage, a constant factor P_F may be used even for different cycles. If necessary, factor P_F may also be derived every time, from the core calculation.

Measured power distribution guess in the directly monitored assemblies is thus obtained by normalising the sum of the values derived, to $\frac{0.97 \times P_F(1-P_F)}{4}$. Factor 0.97 is to take into account of the fact that only 97% of the reactor power appears as heat inside the fuel channel. About 3% of the power is directly deposited in the out channel water by radiations and neutron slowing down.

With the guess of power distribution in all the nodes of monitored fuel assemblies so derived, the coolant flow and void in them are re-calculated. Changed 'D' factors are then estimated (For want of better values, the calculated burnups are again used). We then derive better estimates of the values proportional to fuel node powers. This cycle of calculation is repeated until convergences on void and power distributions are reached. Power peaks and thermal hydraulic parameters like Minimum Critical Heat Flux Ratio (MCHFR) or Minimum Critical Power Ratio (MCPR) are computed using this power and void distribution.

These computations are required often and to be performed quickly during the start up and power escalation of a reactor. An online computer usually performs this job.

(iii) Other Models for Interpretation of TIP Readings in a BWR

Here we had described a somewhat simple model for interpretation of TIP readings in a BWR. One possible deficiency of the model is the assumption that four bundles are separable for finding detector fissions. A more detailed model has been presented by Uchi kawa (1977). For getting the factors similar to 'D' factors that we discussed, he performed four-lattice-cell calculations. These conversion factors are assumed to be a function of both the average void in the four cells and the individual voids in each of them. He and others had also performed subchannel analysis of fuel assemblies to find how the distribution of void inside any channel affect the TIP readings. We had assumed that the void distribution is uniform inside any fuel assembly cross-section. Possibility of small amount of steam generation in the out channel water is also to be considered.

4. RELOAD STRATEGIES

(i) Introduction

Reload strategies form part of the fuel cycle of a power reactor. Fuel cycle consists of fuel material procurement, fuel element fabrication, in-core fuel management, reprocessing and disposal. Reload strategies are essentially the refuelling schemes followed in the in-core fuel management of a reactor. Fuel management is the main theme of next weeks lectures. So this lecture will essentially form a prelude to the more details that you will be hearing in the ensuing week.

As power is derived from the fissions produced in fuel of a reactor, fissile material gets depleted and fission products which are neutron

absorbers accumulate. The physical and metallurgical properties of the fuel element deteriorate due to high temperature operation, neutron irradiation etc. At some stage, old fuel has to be discharged and fresh fuel introduced into the core. The strategies to be followed in removing and introducing fuel is the subject of present lecture. Different types of reactors use different refuelling schemes. Here we will discuss the general fuelling schemes and briefly the refuelling schemes followed in BWRs, PWRs and PHWRs.

In any refuelling scheme, we have to decide the amount of fresh fuel to be loaded as a function of time of reactor operation and guidelines as to where the fresh fuel has tobe located in the reactor core relative to the old fuel. The main aim of any refuelling scheme is to derive as much power as possible from every fuel assembly. The constraints usually encountered are availability of fuel, criticality of reactor, controllability of core reactivity, burnout and fuel temperature limits, metallurgical limits, etc.

Moreover, for any reactor there are normally two phases of the refuelling strategies during its life time of operation. One phase is during the approach to equilibrium and the other during the equilibrium. It is quite possible that true equilibrium in fuelling scheme is never reached. This may be due to factors like changing economic environment, high fuel failure rate, fuel non-availability , plant failure etc. However, the concept of equilibrium cycle is useful for finding guidelines for in-core fuel management.

(ii) General Refuelling Schemes

From a purely reactor physics point of view, when the reactivity of fuel in the reactor is such that reactor becomes only just critical at the required power level, some new fuel has to be introduced for continued operation. This introduction of fuel may be done on power in an almost continuous manner (every day perhaps) as is done in CANDU-PHWRS. The other extreme is the single batch refuelling, where the whole reactor core is replaced in a refuelling as is done in some reactors for special applications. As a compromise, fuelling may be done in batches after a fixed period of time (say every year), as is done in BWRs and PWRs. In the latter two cases, the reactor has to be shut down for every refuelling. The excess reactivity introduced into the core by fresh fuel has to be controlled through proper absorber management.

The discharge burnup of fuel at equilibrium of any reactor depends on the refuelling scheme followed. Let 'N' be the number of refuellings required to completely replace fuel equal to that contained in the reactor core. For continuous refuelling $N = \infty$ and for single batch refuelling N=1. Consider the equilibrium case of continuous refuelling. The reactivity of fuel assemblies under operating conditions in the reactor will have a continuous distribution as shown in Fig. 14 a. It is assumed that reactivity decreases linearly with fuel burnup. Let us denote by K^{o}_{∞} the value of K_{∞} at zero burnup. For the reactor to be just critical with a continuous distribution of fuel burnups, the average value of K_{∞} of all assemblies has to take a value greather than unity, say K^{η}_{∞} (Fig. 14). This value is essentially determined by the neutron leakage from reactor core. The value of K^{η}_{∞} will be larger for smaller cores. The discharge burnup of fuel in the continuous fuelling case is then given by the burnup at which the number of assemblies above K^{η}_{∞} equals the number below it. This is denoted by the value E_{∞}

in the figure. For a given design of fuel assembly, this is the maximum achievable average discharge burnup, for a given reactor core. When the reactor core size increases, the value of k_∞^n comes down and E_∞ increases correspondingly.

Now consider the case of single batch refuelling in the same reactor core. At the start of fuel irradiation, all fuel assemblies are assumed to have multiplication factor K_∞^0. After a core burnup of $E_\infty/2$, the average K_∞ value of all the assemblies would have fallen to K_∞^n. The average burnup of discharged assemblies in single batch refuelling is only half of that achievable with continuous refuelling.

Let E_N be the discharge burnup of fuel assemblies in the case of N batch refuelling scheme at equilibrium. $\frac{1}{N}$ fraction of the fuel in the core is discharged at average burnup of E_N at every refuelling. The equilibrium cycle length has to be $\frac{E_N}{N}$. Consequently the burnup distribution of fuel assemblies at the end of cycle (EOC) has to be as follows. At EOC, N equal batches of fuel assemblies will be present in the core, with batch average burnups of

$$\frac{E_N}{N}, \frac{2E_N}{N}, \ldots\ldots\ldots \frac{(N-1)E_N}{N}, E_N$$

The batch of fuel assemblies having average burnup E_N accumulated through irradiation in N cycles, is to be discharged.

At the EOC, the average K_∞ value of assemblies has to be K_∞^n below which the reactor becomes subcritical at the rated power. This happens when core average burnup reaches $\frac{E_\infty}{2}$

Hence
$$\frac{E_\infty}{2} = \frac{1}{N}\sum_{i=1}^{N} i\frac{E_N}{N} = \frac{N+1}{N}\frac{E_N}{2}$$

The equilibrium discharge burnup in N batch refuelling E_N, is then given by
$$E_N = \frac{E_\infty \times N}{N+1}$$

Equilibrium cycle length is $E_\infty/(N+1)$. This means that the distribution of fuel assembly burnups at the Beginning of a Cycle (BOC) consists of groups of assemblies having average burnups

$$0, \frac{E_N}{N}, \ldots\ldots\ldots \frac{(N-1)E_N}{N}$$

The above described burnup distribution at EOC core is illustrated in Fig. 14 b. The loss in discharge burnup in N batch refuelling compared to the continuous refuelling is also $\frac{E_\infty}{N+1}$. The loss is small for large value of N. In LWR, the reactor has to be shut-down for a certain period of time for every refuelling, resulting in loss of power generation. A balance will have to be made between these two losses for choosing a suitable batch refuelling scheme. It is found that three to five batch refuelling is optimum.

In case of batch refuelling, it is possible to recognize two basic ways of positioning fresh fuel in the core relative to the burned fuel. In the out-in scheme, fresh fuel is introduced at the core

periphery and the less burned fuel in the adjacent outer ring and the most burned fuel at core centre. This leads to power flattening at the expense of reduced utilisation of fuel. More cycle length could have been achieved if fresh fuel is positioned inside the core.

The other extreme is the in-out scheme where fresh fuel is loaded at the centre of core and fuel burnups increase progressively as we proceed to the core periphery. This scheme utilises fresh fuel efficiently in their first cycle, but will lead to power peaking which may be excessive.

(iii) Refuelling Schemes in a BWR

The refuelling scheme followed in a BWR is a mid way course between in-out and out-in refuelling schemes. Originally it was envisaged to follow a checker board scheme where the four fuel assemblies surrounding a cruciform control rod approximately have burnups corresponding to fresh, one cycle burned, two cycle burned and three cycle burned assemblies. Such a distribution through out the core with the restriction that the fresh assemblies are not located in the very periphery or very centre of the core , gives a good balance between power flattening and fuel utilisation.

With experience, this refuelling scheme has been improved upon as shown in Fig. 15. The distribution of K_{∞} values of fuel assemblies in the core is shown as a function of distance from the core centre. The important modifications from the original checker board scheme are that the highly burned fuel is located in the very periphery and the fresh fuel is located in a region closer to the periphery. The fuel assembly powers in the periphery are dictated by neutron leakage. Hence the positioning of highly burned fuel in periphery increases the utilisation of less burned fuel inside and at the same time reduces neutron leakage due to lesser flux level at the periphery. The positioning of fresh fuel away from centre reduces the radial power peaking.

When burnable poison is present in BWR fuel, the variation of K_{∞} value with burnup is no longer linear. But the amount of burnable poison is adjusted such that it burns out in one cycle of burnup (ie $\frac{E_N}{N}$). Hence our arguments regarding discharge burnup in N batch refuelling remain valid. The modified refuelling scheme discussed in Fig. 15 remains valid with the change that fresh fuel is to be understood as highest reactivity fuel which now becomes the one cycle burned fuel.

Refuelling schemes in initial cycles will usually be different. Initial core design may contain less enriched fuel than the one planned for equilibrium cycle and some may have higher concentrations of burnable poison. Natural uranium fuel assemblies may be used for periphery. Fuel assemblies discharged at the end of first cycle will have burnups much less than the equilibrium discharge burnup. Hence these fuel assemblies are reinserted in later cycles.

(iv) Refuelling Schemes in a PWR

The typical equilibrium refuelling scheme for PWRs is a three batch out-in scheme. The underlying principles are the following,

(a) the core is divided into two zones

(b) fresh fuel assemblies are located at the core periphery and

(c) the partially depleted fuel assemblies which have been irradiated for one or two cycles are distributed in the inner zone using a checker board scheme.

The emphasis is on power flattening using fuel assembly burnups, as the finger type control rods are usually not used during reactor operation. Boron poisoning of the moderator is used to control the reactor during power operation. The cycle ends when the boron poison goes to zero.

In the approach to equilibrium cycle, deviations occur from the equilibrium cycle. To attain power flattening in the first cycle itself, enrichment variation of fuel assemblies is used. Fuel of enrichment planned for equilibrium cycle is loaded in the core periphery. Fuel assemblies of two lower enrichments are located in a chcker board pattern in the centre zone of the core. Burnable poison is usually used in the initial core. Reinsertion of fuel assemblies discharged in first cycle may be contemplated during the approach to equilibrium cycles.

(v) Refuelling Schemes in a PHWR

The CANDU-PHWRs are fuelled with natural uranium continuously and on power. Thus the fuel utilisation is much better here compared to LWRs. As described by earlier lecturers, the reactor axis is horizontal and fuel channels form a square lattice. Each channel contains usually 12 fuel bundles. To get flat axial flux shape, half the channels are fuelled from one side and the other half from the opposite side. One channel fuelled in one direction has four nearest channels fuelled in opposite direction. Four or eight fuel bundles may be loaded into one channel at a time and the same number of depleted fuel bundles removed from the other end of the channel. Each bundle moves in steps along one end of channel to the other during its irradiation life.

Two bundle shifts were initially used for any refuelling. These were later replaced by eight bundle shifts to avoid frequent use of fuelling machine and to give lesser power shock to the shifted fuel. However there was a resultant loss of burnup in discharged fuel. With better fuelling machine and fuel design, the four bundle shifts are being considered now. In the equilibrium refuelling scheme, there are two burnup zones in the reactor. To achieve radial power flattening, the fuelling rate in the centre zone is lower than in the outer zone. Consequently the discharge burnup of fuel bundles in the central zone is greater. Refuelling is done to maintain reactor critical at the rated power level.

In approach to equilibrium cycle there may be deviations from the equilibrium fuelling scheme. If depleted fuel as assemblies from previous reactors are available, then equilibrium fuelling can be established in CANDU-PHWRs quickly. However, if such depleted fuel is not available complications in fuelling scheme occur. With a all fresh natural uranium core it is not possible to achieve full power in the beginning due to the non availability of radial control elements for reducing the consequent power peaking at the core centre. With core burnup, the power distribution flattens and the reactor power can be increased. To reach the full power in a reasonable time, refuelling at the core periphery should be made at a faster rate than the centre. Discharged fuel bundles will have less than the desired burnup and can be reinserted in other channels or in other reactors.

REFERENCES

1. Tyror J.G. (1973), Reactor Burnup Physics- Developments in the Physics of Nuclear Power Reactors- IAEA Technical Reports Series No.- 143.
2. Unik J.P and Gindler J.E. (1971) A Critical Review of the Energy Released in Nuclear Fission, USAEC report-ANL- 7748.
3. Cuninghame J.G. (1977), The Status of Fission Product Yield Data in 1977, IAEA Panel, Petten, Netherlands.
4. Rider B.F and Meek M.E. (1978), NEDO-12154-2E.
5. Ottewitte E.H. (1977), Significance of the Expanded Xenon and Samariam Decay Chain Information, TANS, 27, 921.
6. Zolotar B.A. (1979), Nodal Methods for Utility Applications, Paper presented at the NEACRP Specialists Meeting on Calculation of 3-Dimensional Rating Distributions in Operating Reactors, Paris.
7. Askew J.R. et al, (1966) A General Description of the Lattice Code WIMS, J. of BNES 5, 584.
8. Huria H.C. (1978), MURLI-A Multigroup Integral Transport Theory Code for Thermal Reactor Lattice Studies, ATKE-31, 87.
9. Fayers F.J. et al (1972) LWR- WIMS. A Modular Code for Evaluation of LWR Lattices AEEW-R 785.
10. Nephew E.A. (1960), Thermal and Resonance Absorption Cross-Sections of the ^{233}U, ^{235}U and ^{239}Pu Fission Products, ORNL- 2869.
11. Critoph. E. (1978), Reactor Physics Aspects of CANDU Reactors. Lecture Series at the Winter Course in Reactor Theory and Power Reactor ICTP, Trieste.
12. Uchikawa.S. (1977), Experimental Verification of a Method for Simulating a Boiling Water Reactor Core Based on Few Group Coarse Mesh Diffusion Scheme. Nucl. Tech. 33.

TABLE - I

ENERGY IN MeV DEPOSITED IN EBR-II REACTOR PER FISSION FOR DIFFERENT HEAVY NUCLIDES.

Nuclide	Q_f	E_ν	Q_γ	Q_T
^{232}Th	196.37	13.3	8.88	192.0 ± 1.0
^{233}U	197.99	7.8	9.71	200.0 ± 0.6
^{235}U	202.74	10.3	9.29	201.7 ± 0.7
^{238}U	205.39	14.7	11.82	203.0 ± 1.1
^{239}Pu	207.16	8.8	12.26	210.6 ± 0.7
^{240}Pu	206.4	10.1	14.17	210.5 ± 2.2
^{241}Pu	210.92	11.5	12.63	212.0 ± 0.8
^{242}Pu	210.8	12.9	14.24	212.1 ± 4.2

Q_f - fission energy release

E_ν - anti neutrino energy

Q_γ - neutron capture γ-ray energy

Q_T - energy deposited in the reactor

TABLE - II

FUEL COMPOSITION CHANGE WITH BURNUP

	BWR Fuel		PHWR Fuel	
	BOL	EOL	BOL	EOL
^{235}U	0.024	0.007	0.007	0.0015
^{238}U	0.976	0.984*	0.993	0.994*
^{239}Pu	0	0.005	0	0.0027
^{240}Pu	0	0.002	0	0.0013
^{241}Pu	0	0.001	0	0.0003
^{242}Pu	0	--	0	0.0001
Pu/U	0	0.008	0	0.0043
Fissile Pu · Fraction	0	0.69	0	0.68

* Value increased due to 2_{200}-normalization

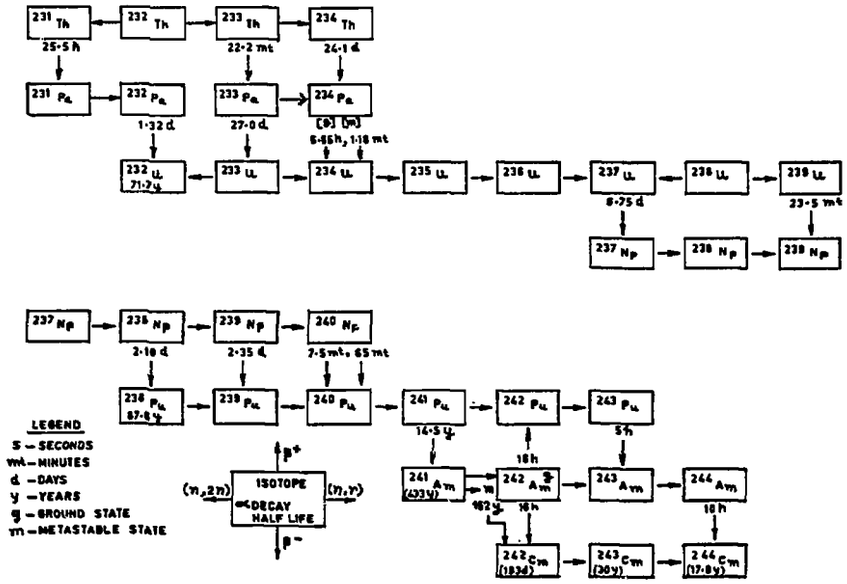

FIG. 1. DEPLETION AND BUILDUP CHAINS OF ACTINIDES

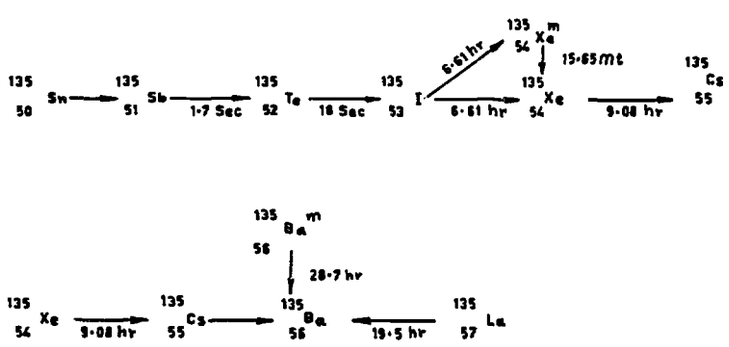

FIG. 2. EXPANDED XENON DECAY CHAIN

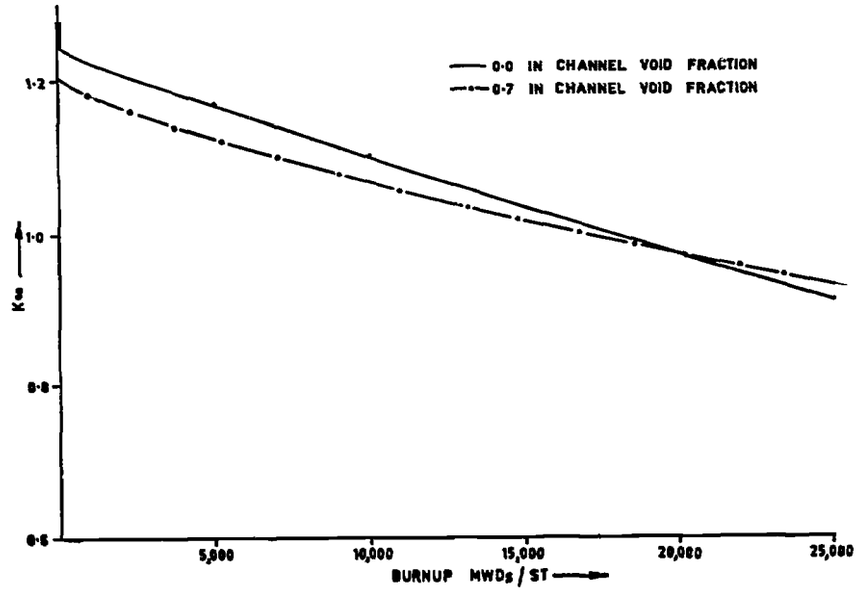

FIG. 3. K_∞ VARIATION WITH BURNUP FOR A BWR FUEL BUNDLE

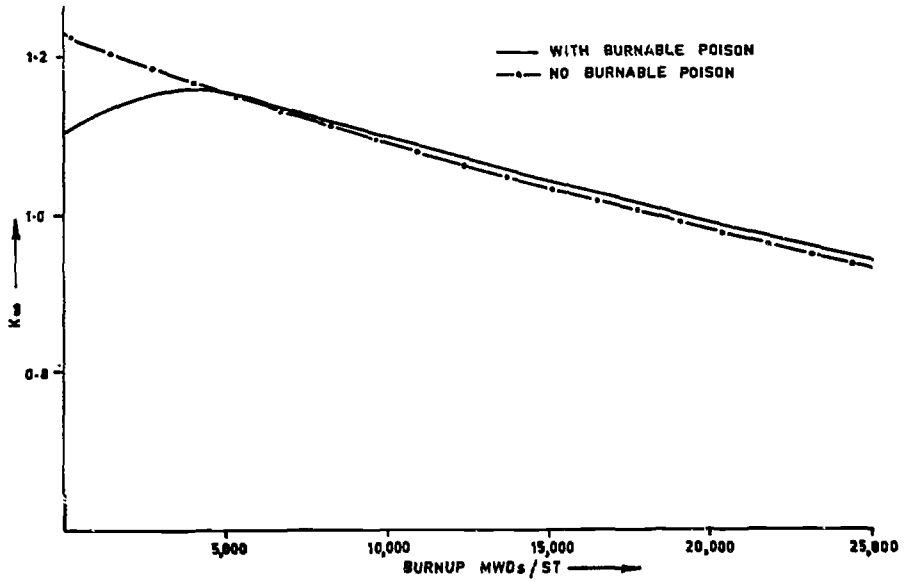

FIG. 4. K_∞ VARIATION WITH BURNUP FOR A BWR FUEL BUNDLE WITH AND WITHOUT BURNABLE POISON (IN CHANNEL VOID FRACTION = 0·4)

BUNDLE BURNUPS AT BEGINNING OF CYCLE (IN MWDs/ST)		BUNDLE BURNUPS TOWARDS END OF CYCLE (IN MWDs/ST)	
0·0	4,500	4,500	9,000
4,500	0·0	9,000	4,500

BUNDLE K_∞S AT BEGINNING OF CYCLE		BUNDLE K_∞S TOWARDS END OF CYCLE	
1.105	1.157	1.157	1.107
1.157	1.105	1.107	1.157

FIG. 5. USE OF BURNABLE POISON IN POWER FLATTENNING

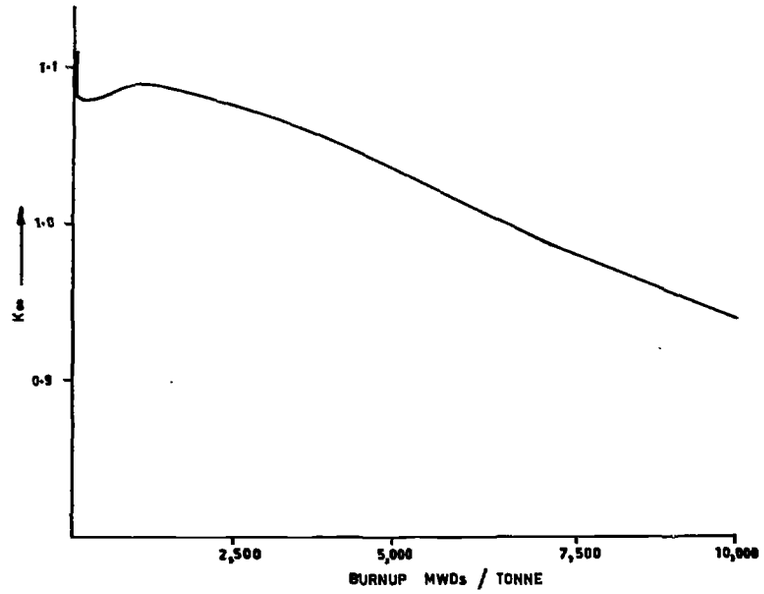

FIG. 5. K_∞ VARIATION WITH BURNUP FOR PHWR FUEL BUNDLE

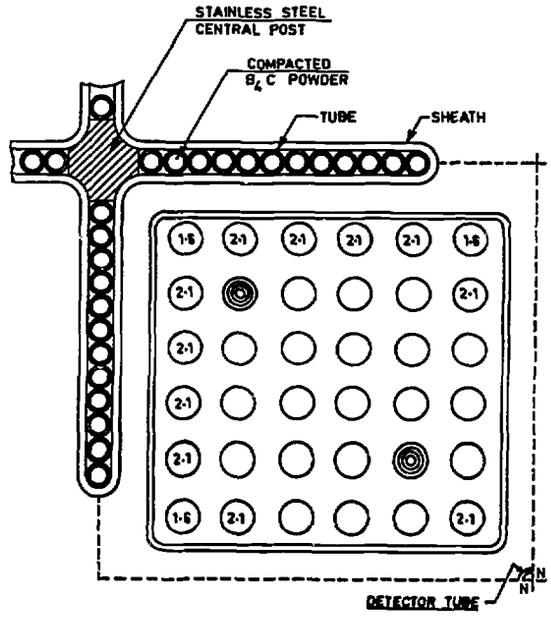

FIG.7 TARAPUR LATTICE UNIT CELL

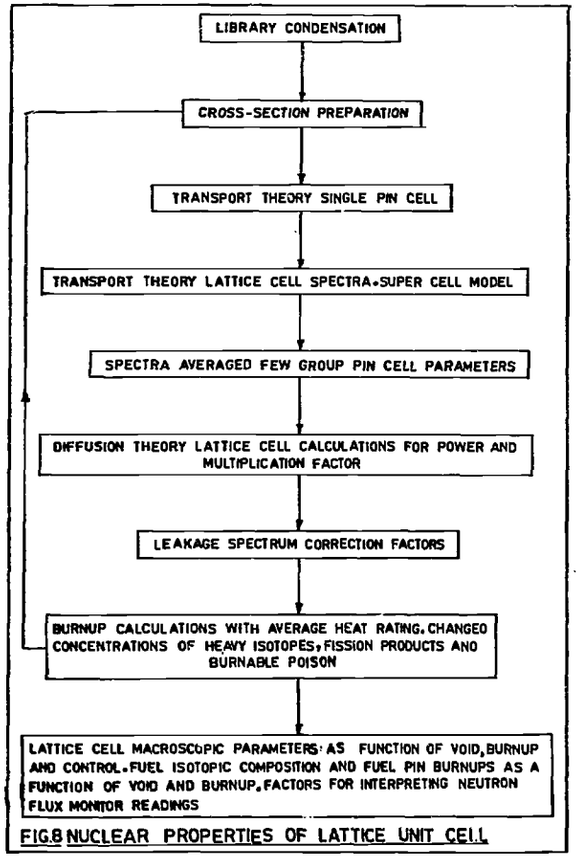

FIG.8 NUCLEAR PROPERTIES OF LATTICE UNIT CELL

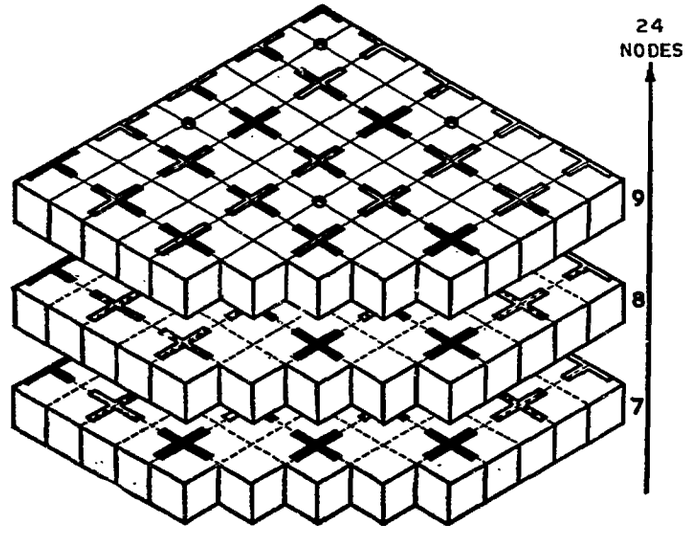

TOTAL NO. OF NODES = 284 X 24 = 6816

FIG. 9 TARAPUR 3D SIMULATION

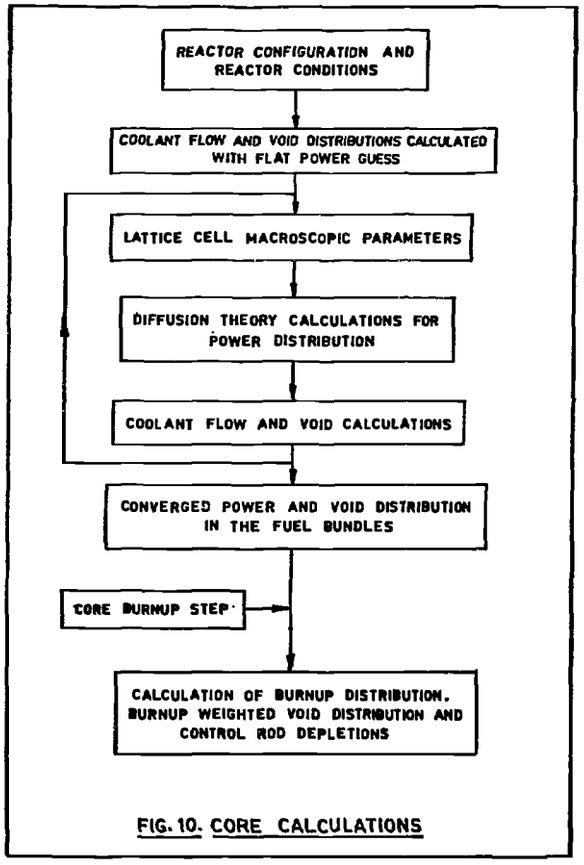

FIG. 10. CORE CALCULATIONS

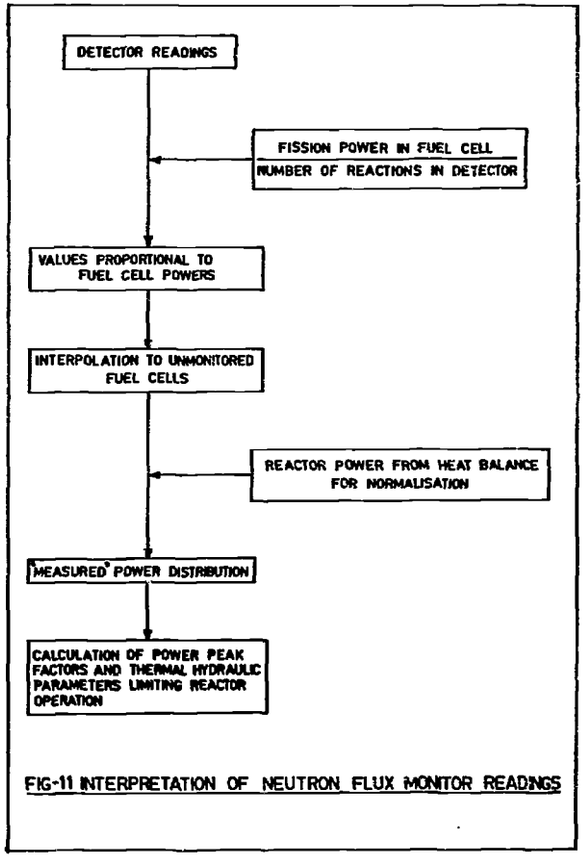

FIG-11 INTERPRETATION OF NEUTRON FLUX MONITOR READINGS

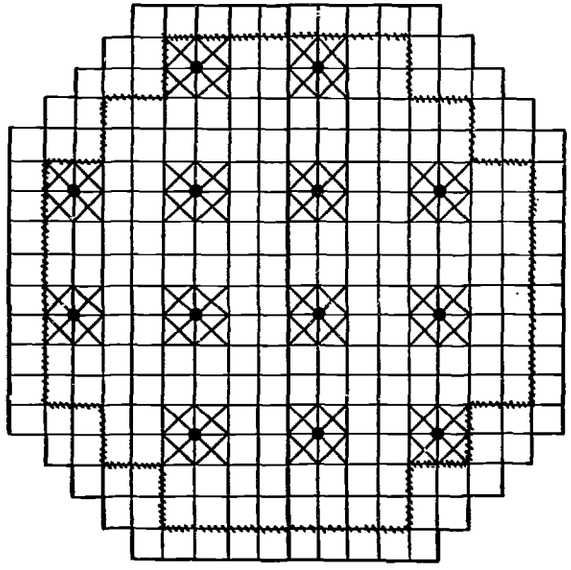

FIG12-TIP DETECTOR LOCATIONS AND MONITORED FUEL CELLS IN A BWR

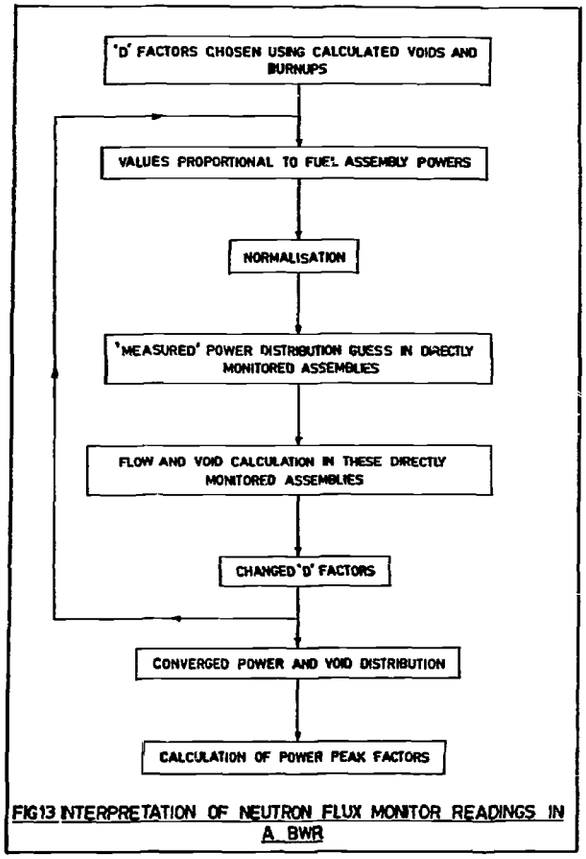

FIG13 INTERPRETATION OF NEUTRON FLUX MONITOR READINGS IN A BWR

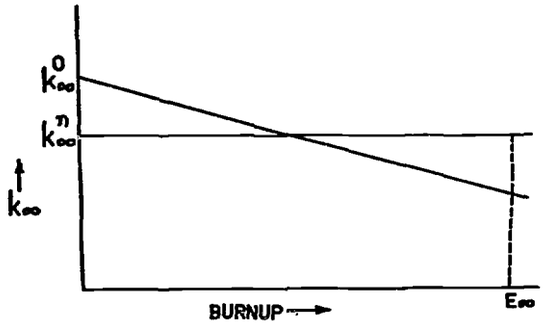

(a) CONTINUOUS REFUELLING

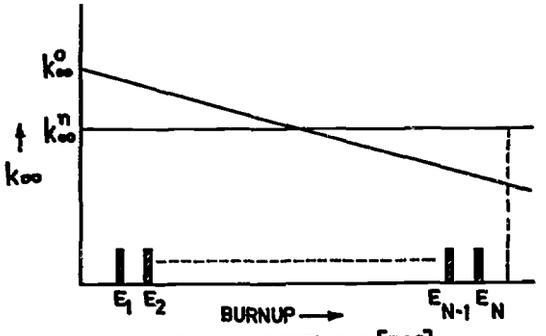

(b) BATCH REFUELLING [EOC]

FIG.14 BURNUP OF DISCHARED FUEL

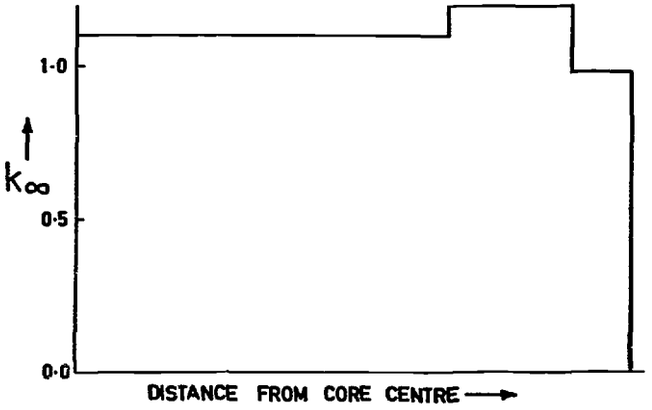

FIG.15 DISTRIBUTION OF ASSEMBLY k_{∞} VALUES IN A BWR REFUELLING SCHEME